

## Polyaniline Nanofiber Embedded with $Y_2O_3$ Composites Doped with Dodecyl Benzene Sulfonic Acid, Characterization and Electrical Properties

### Abstract

Polymer nanocomposites of polyaniline nanofiber/Green synthesized  $Y_2O_3$  (Pani/Gs  $Y_2O_3$ ) are synthesized by in situ polymerization using dodecyl benzene sulfonic acid as a surfactant media. The Gs  $Y_2O_3$  is dispersed in 1, 3, 5 and 7 weight percentages in Pani to give Pani/Gs  $Y_2O_3$  composites. The Pani/Gs  $Y_2O_3$  composites are characterized by Ultra Violet, Infra-Red spectroscopy and X-ray diffraction techniques. The SEM and TEM image shows the fibrous morphology of the composite. Pani nanofiber/5%Gs  $Y_2O_3$  nanocomposites show highest frequency dependent conductivity, dielectric constant and dielectric loss Properties at room temperature. Such a polymer composites have EMI shielding, sensor and battery applications.

**Keywords:** Mushroom, Yttrium oxide, Combustion synthesis, electrical conductivity, Solution combustion synthesis dielectric constant.

Satishkumar KB<sup>1</sup>,  
Vishnuvardhan TK<sup>\*2</sup>,  
Shashidhar<sup>3</sup>,  
Murugendrappa MV<sup>4</sup>,  
Rajashekhhar B<sup>5</sup>

### Author Affiliations

<sup>1</sup>Department of Chemistry, Acharya Institute of Technology, Achith Nagar, Soladevanahalli, Bangalore 560 107, India.

<sup>2</sup>Department of Chemistry, Ramaiah University of Applied Sciences, Peenya Campus, Bangaluru 560 058, India

<sup>3,5</sup>Department of Chemistry, SDM College of Engineering and Technology, Dharwad 580 002 India.

<sup>4</sup>Department of Physics, BMS College of Engineering, Bull Temple Road, Bangaluru 560 019, India.

### \*Corresponding Author

Vishnuvardhan TK,  
Department of Chemistry, Ramaiah University of Applied Sciences, Peenya Campus, Bangaluru 560 058, India

E- mail: vishnu33vardhan@gmail.com

Received on 05.07.2019

Accepted on 12.09.2019

### 1. Introduction

Synthesis of metal oxide is fascinating to modify the crystal structure, morphology to tailor the unique properties. Synthesis of such oxide by co precipitation<sup>1</sup>, solvo- thermal<sup>2</sup>, hydrothermal<sup>3</sup>, sol-gel method<sup>4</sup>, combustion<sup>5,6</sup> and bio synthesis<sup>7</sup> are more commonly found in literature. Morphologies of such synthesized oxides show cubic, orthorhombic or different crystal structure, morphology provide the large surface energy; thereby found application in optics, phosphorescence and fluorescent active materials etc. Yttrium oxide synthesized by solution combustion method using different fuel and combustion temperature provides the various morphological features<sup>8</sup>. In combustion method fuel will be different organic compound containing N, S and C functional groups isolated possess same constituents in different living systems<sup>9</sup>. Several reports show the different plant parts are used as a source of fuel in combustion synthesis of nanoparticles also changes the morphology and exploiting the properties of such composites<sup>10-12</sup>. Silver and gold nano particles are

synthesized using the *Agaricus Bisporous* extract<sup>13</sup>, biosynthesis<sup>14</sup> etc., in our earlier report optimized synthesis of  $\text{Y}_2\text{O}_3$  nanoparticles using mushroom *Agaricus Bisporous* by solution combustion method forms needle like morphology is reported<sup>15</sup>.

Effect of polymerization of aniline on the oxidant  $\text{FeCl}_3$  and its morphology has much impact on the conductivity<sup>16</sup>. They compared the conductivity of Pani film and powder, reported that as the Pani film has high conductivity due to increase in the molar ratio of Pani/oxidant increases the thickness of the film, however, over oxidation of the Pani, due to the increase in the oxidant concentration also reported. Prepared film shows better volatile organic vapour sensor active due to porous structure. High sensitivity of the Pani film is due to porous structure can provide larger surface area for the easy diffusion of the volatile organic compounds in comparison with the compact Pani film. They also reported thermal and electrical properties of the Pani prepared by  $\text{FeCl}_3$  has less than that of the Pani prepared by Ammonium peroxy disulfate (APS) as oxidant. Preparation of Pani nanofibers and its composite preparation can more predominantly found with APS<sup>17,18</sup> and <sup>20</sup>.

In spite of the above  $\text{FeCl}_3$  and APS as independent oxidants in the Pani preparation, there is mixed composite oxidant in presence of Dodecyl Benzene Sulphonic Acid (DBSA)<sup>19</sup>. Preparation of polyaniline nanofibers using co-oxidants of APS and hypochlorites, they found that due to the addition of the co-oxidant hypochlorite along with APS produces the longer length and thinner nanofibers gives higher conductivity which is higher than the conductivity of Pani prepared by APS alone as oxidant. Studies also confirm the mere APS alone do not influence the formation of the Pani nanofibrous. Reducing the concentration of aniline giving the fibrous nature of the Pani<sup>18</sup>. Polyaniline nanofibrous are generally obtained using surfactant media is provided in the literature, recently without using the surfactants polyaniline chain like hallow spheres are reported<sup>20</sup>. Adjustable chain length and shell thickness can be achieved using amino  $\text{Fe}_3\text{O}_4$  coated with polyaniline. Morphology of such synthesized Pani shows microsphere chains in  $\text{FeCl}_3$  media. Increase in the concentration of HCl, growth of the chain increases on amino  $\text{Fe}_3\text{O}_4$  microspheres due to hydrogen bonding<sup>20</sup>.

The electrical properties of the polymer/ $\text{Y}_2\text{O}_3$  nanocomposites vary with the synthesis, with variation of the media, concentration of dopant, oxidant etc. Synthesized metal oxides are also added during the polymerization with different monomers, mainly Pani/ $\text{Y}_2\text{O}_3$ <sup>21-23</sup>, PPy/ $\text{Y}_2\text{O}_3$ <sup>24-25</sup> and Graphene/ $\text{Y}_2\text{O}_3$  quantum dot<sup>26</sup> composites.

This work presents preparation of Gs  $\text{Y}_2\text{O}_3$  by combustion of Yttrium nitrate and *Agaricus Bisporous* as a fuel heated to 375-400 °C in a furnace yields a white powder called as Gs  $\text{Y}_2\text{O}_3$ . Polyaniline prepared by using DBSA with mixed oxidant ( $\text{FeCl}_3$ +APS) shows the nanofibrous morphology. Gs Nano  $\text{Y}_2\text{O}_3$  is used in 1%, 3%, 5% and 7 weight percentages is added during the in situ polymerization of aniline to form Pani/1%Gs $\text{Y}_2\text{O}_3$ , Pani/3% Gs  $\text{Y}_2\text{O}_3$ , Pani/5% Gs  $\text{Y}_2\text{O}_3$  and Pani/7% Gs  $\text{Y}_2\text{O}_3$  composites. Above synthesized composites are characterized by UV, FTIR, XRD, morphology of the composites are studied by SEM and TEM. Results of electrical properties of the Polyaniline nanofiber/ Gs  $\text{Y}_2\text{O}_3$  composites are reported.

## 2. Materials and Methods

### 2.1 Materials

Ammonium Peroxydi Sulfate (APS) from Fischer (AR-grade), Yttrium oxide synthesized in the lab using *Agaricus Bisporus* as oxidant for nanoyttria and Aniline and Surfactant as DBSA were obtained from Fluka and used in the present study. Aniline monomer was purified by distillation under reduced pressure and stored at 4°C in the absence of light.

UV-Vis spectrophotometer model Agilent Technologies of Cary60 spectrophotometer with wavelength range 200 –600 nm. The FTIR model used for our characterization is Tensor 27 Bruker 164, Room temperature FTIR spectra in KBr medium with the range of 4000–600  $\text{cm}^{-1}$  is used for characterization. The composites were analysed by powder X-ray diffraction pattern using

Shimadzu(MAXima\_XRD-7000) using  $\text{CuK}\alpha$  radiation range  $10\text{--}80^\circ$   $\lambda = 1.5406 \text{ \AA}$ . Morphology of the Pani and Pani/Gs.  $\text{Y}_2\text{O}_3$ composites were investigated by using Hitachi-3000 and Transmission electron Microscopy(TEM, TECNAIF-30).

The compressed Pani, Pani/Gs  $\text{Y}_2\text{O}_3$  composite pellets by a standard four-probe method at room temperature using a Keithley 196 System DMM Digital Multi-meter and an Advantest R1642 programmable dc voltage/Current generator as the current source.

### 2.2 Preparation Pure Gs $\text{Y}_2\text{O}_3$

Homogeneous solution of precursor yttrium nitrate hexa hydrate is mixed in minimum amount of nitric acid and stirred thoroughly in a silica crucible. Optimized precursor solution to fuel (thoroughly dried and ground *Agaricus Bisporous*) ratio of 1:1.5 is taken in silica crucible<sup>15</sup>. Silica crucible containing the above mixture is heated to 375-400 K in muffle furnace. When the temperature of the solution goes beyond the 373K solution begin to boil and forming foam with liberation of gases, fumes ceases indicate the formation of stable compound with the foamy yellowish mass is placed in furnace and heated to 500  $^\circ\text{C}$  for 3-4 hrs to get white powder as  $\text{GsY}_2\text{O}_3$ .

### 2.3 Preparation of Pure Pani

Dissolving 0.2 mole of aniline of 500 ml 1N HCl solution with oxidants of APS +  $\text{FeCl}_3$  of 0.2 mole each solution and then slowly mixing these solutions using Magnetic stirrer kept at 400rpm, The whole reaction mixture is surrounded by an ice-bath (maintained at  $0\text{--}5^\circ\text{C}$ ), a chemical oxidative polymerization process was taken for 3.0h. The precipitate was filtered and washed by methanol and distilled water.

### 2.4 Preparation of Pani/Gs $\text{Y}_2\text{O}_3$ nanocomposite

Polyaniline is Chemically polymerized by using 0.2 mole aniline monomer was added drop wise to the aqueous solution of 100 ml of Ammonium peroxydisulphate +  $\text{FeCl}_3$  (0.2 mole each) solution as mixed oxidant in acid medium (1 N) HCl. Surfactant DBSA of about 1 g are added to above mixture with stirring for 4-5 hour using magnetic stirrer with stirring rate 400 rpm. Reaction mixture was maintained at  $0\text{--}5^\circ\text{C}$ . During this process molecular level mixing of precursor aniline and the polymerization of initiators (APS +  $\text{FeCl}_3$ ) resulting in the polymer chain networks. The 1, 3, 5 & 7 weight percentages of yttrium oxide is added to the above solution during polymerization. The Aniline oxidises with  $\text{FeCl}_3$  and APS solution, after an induction period of about 10 min in presence of DBSA. The completion of polymerization can be achieved by adding mixed oxidizing agent and the reaction mixture turns to dark blue to green emeraldine<sup>27</sup>. To achieve maximum dispersion of yttrium oxide in the polymer solution the reaction mixture was stirred for about 4 h. After 4 h of stirring, the Pani/ Gs  $\text{Y}_2\text{O}_3$  (Pani/1% Gs  $\text{Y}_2\text{O}_3$ , Pani/3% Gs  $\text{Y}_2\text{O}_3$ , Pani/5% Gs  $\text{Y}_2\text{O}_3$  and Pani/7% Gs  $\text{Y}_2\text{O}_3$ ) was washed thoroughly with methanol to remove unreacted aniline and followed by distilled water. Above composites were vacuum dried at  $60\text{--}70^\circ\text{C}$  for 1 h.

## 3. Result and Discussion

### 3.1. UV visible

UV-Visible absorption spectra of Pani and Pani/ Gs $\text{Y}_2\text{O}_3$  nanocomposites in alcohol media are given in Fig. 1. Pani/ Gs  $\text{Y}_2\text{O}_3$  nano-composites absorb the UV and visible light. The characteristic the polyanilinium cation, fork like peak obtained at 205 and 221 nm for pure Pani in the spectrum<sup>28</sup> indicating the doped form of the polyaniline<sup>29</sup>.

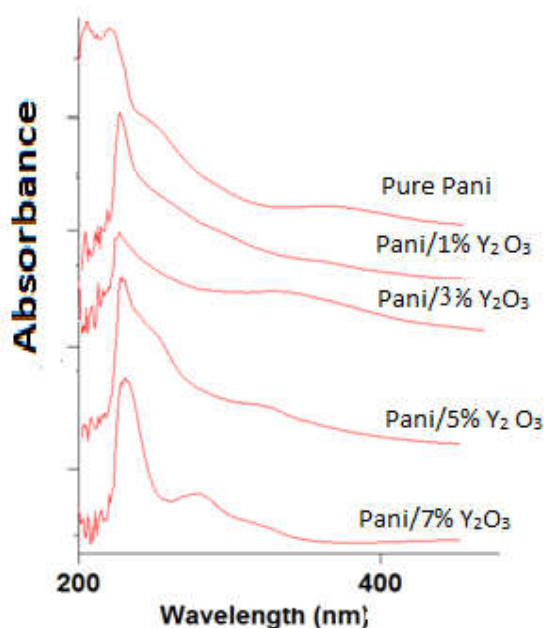


**Figure 1:** Shows the UV visible spectra of Pani/ Gs  $Y_2O_3$  nanocomposites inset for Pure Pani

The sharp peak in the composites is recorded at 227 nm for Pani/1% and 3% Gs  $Y_2O_3$  composites show 228 nm and 231,290 for Pani/5% and Pani/7% Gs  $Y_2O_3$  composites respectively. As the  $Y_2O_3$  percentage increases in the Pani there is shift towards higher absorption wavelength region for the Pani/Gs  $Y_2O_3$  composites. As the concentration of the  $Y_2O_3$  increases intensity of the peak variation indicates the effects of  $Y_2O_3$  in the composites<sup>8</sup>.

The Pani/ Gs  $Y_2O_3$  composites shows additional small peak at the 290nm for Pani/ 7% Gs  $Y_2O_3$  and that of Pani /5% Gs  $Y_2O_3$ , Pani/ 3% Gs  $Y_2O_3$  composites shows 330 nm, and 390 nm respectively. These peaks in the UV visible may be due to the conversion of aniline into oxidized form of the polyaniline, these oxidised form of the polyaniline is well match with literature<sup>30</sup>.  $\pi$ - $\pi^*$  transition of the benzene ring of the Pani showing in the form of emeraldine salt this is well match with literature<sup>20</sup>.

Dispersion of Gs  $Y_2O_3$  increases as 1%, 3%, 5% and 7%  $Y_2O_3$  in Pani/ Gs  $Y_2O_3$  nanoparticles are found. Due to their high molar mass of  $Y_2O_3$ , in the Pani/7%  $Y_2O_3$  composites, additional small peak at 290 nm may be due to the scatter of  $Y_2O_3$  particles. The intensity of scattered light from  $Y_2O_3$  smaller than or comparable to the wavelength of light of Pani is inversely proportional to the fourth power of wavelength<sup>30</sup>. Increase of absorbance 290 nm can thus be affected by the formation of dispersion of weight percentage of  $Y_2O_3$  particles proportional with polyaniline.

### 3.2 FT IR

Fig. 2: indicates the FTIR spectra of Pani/Gs  $Y_2O_3$  composites. FT-IR spectra of pure Pani. Characteristic absorption peaks at  $1539\text{ cm}^{-1}$  ranges in the composites corresponds to the C-C and C = C stretching vibrations. The characteristic peaks of the Pani molecules in the composite are shifted to lower wave number compared with those of pure Pani ( $1558\text{ cm}^{-1}$  Inset) as shown in Fig.2.

The presence of  $Y_2O_3$  in the Pani/Gs  $Y_2O_3$  composites is confirmed from IR spectra, which showed absorptions at  $675\text{ cm}^{-1}$ , characteristic of Y-O stretching<sup>8</sup>. In pure Gs  $Y_2O_3$  it is noticed at  $681^{15}$ . As the

concentration of Gs  $\text{Y}_2\text{O}_3$  increases small shoulder like absorption peak indicating the encapsulation of the Pani on the Gs  $\text{Y}_2\text{O}_3$ . At lower concentration dispersion is more with more encapsulation. In case of higher concentration of Gs  $\text{Y}_2\text{O}_3$  coating of Pani is less, indicated with less intensity of the peak. Presence of intense 1229 and 989  $\text{cm}^{-1}$  peaks for Pani/ 5% and 7% Gs  $\text{Y}_2\text{O}_3$  indicate the oxidized form of the polyaniline<sup>31</sup>nanofibre formation. From this it conclude that there is an interaction between Pani nanofibre and the Gs  $\text{Y}_2\text{O}_3$  nanoparticles in the composites.

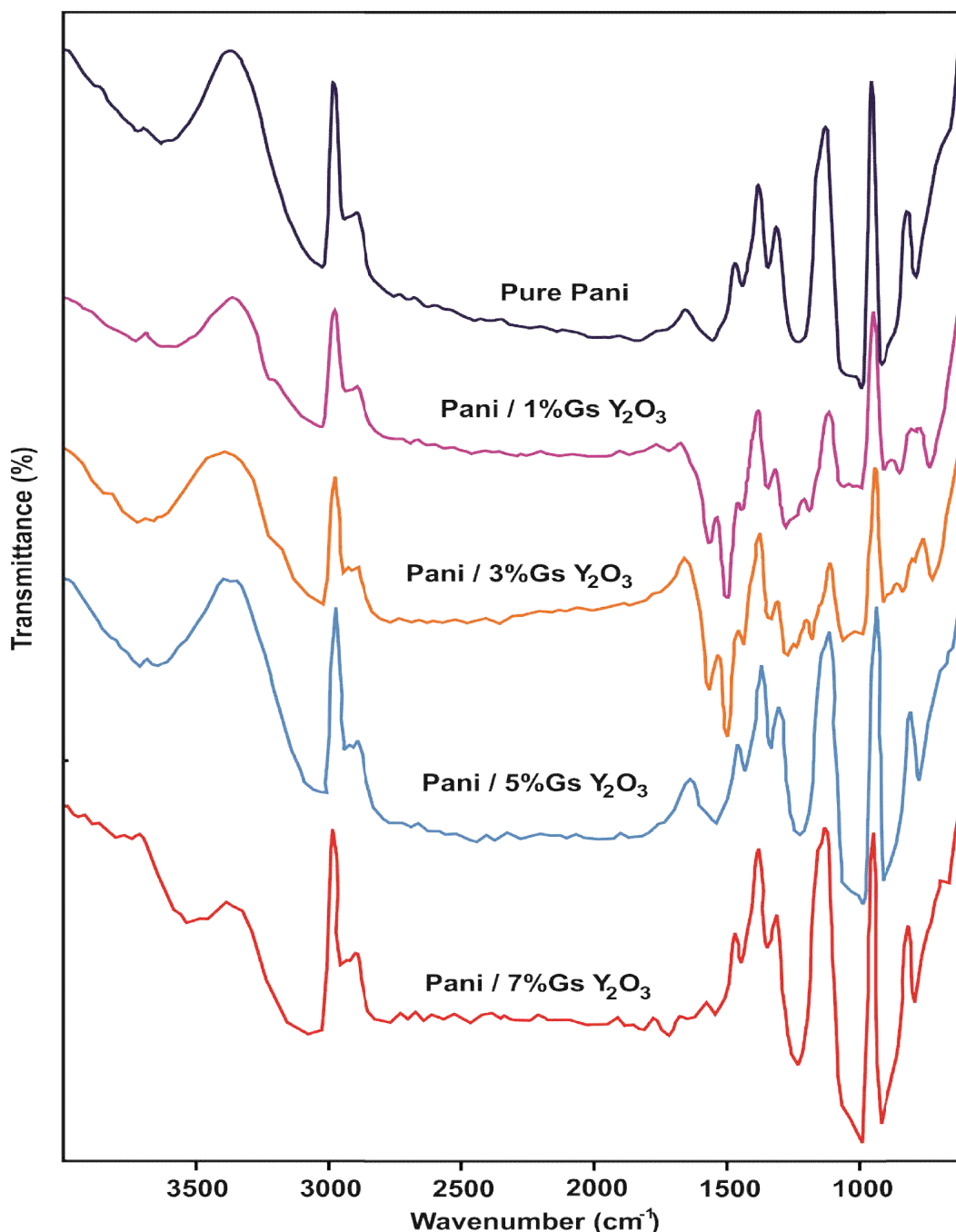


Figure 2: Shows the FTIR spectra of Pure Pani and Pani/ Gs  $\text{Y}_2\text{O}_3$  nanocomposites

### 3.3 XRD

Fig. 3a presents X-ray diffraction pattern of pure Pani and Fig. 3 b-e presents Pani/ Gs  $\text{Y}_2\text{O}_3$  (1,3,5 and 7 weight %) composites, doped Pani nanofibers oxidized by  $\text{FeCl}_3$  and APS, Sharp peaks and their planes are given in the table 1 values are matching with the literature for the monoclinic space group P21,<sup>32,34</sup>. The XRD curve of the PANI nanofibers oxidized by mixed oxidants shown in the table, two peaks centred at  $2\theta = 20.18$  and  $25.28$ , which is in agreement with literature<sup>34</sup>. Thus, Fig. 3 also indicates that the crystalline polyaniline nanofibers oxidized by  $\text{FeCl}_3 + \text{APS}$  at lower  $2\theta$  values i.e upto  $2\theta = 25^\circ$ . Characteristic broad peak of amorphous polyaniline<sup>35</sup> is due to the scattering from Pani chains at inter planar spacing [36]. The appearance of the sharp peaks above  $2\theta = 30^\circ$  in the 1%, 5% and 7% Pani/Gs  $\text{Y}_2\text{O}_3$  composite may indicate degree of crystallinity in the composite may be due to the presence of  $\text{Y}_2\text{O}_3$ . These characteristics planes of Gs  $\text{Y}_2\text{O}_3$  in the composite well matches with the JCPDS file No. 88-1040 and literature<sup>8 and 15</sup>. In case of Pani/3% Gs  $\text{Y}_2\text{O}_3$  composites characteristic  $\text{Y}_2\text{O}_3$  planes are not so pronounced may be due to encapsulation of pani on the  $\text{Y}_2\text{O}_3$ .

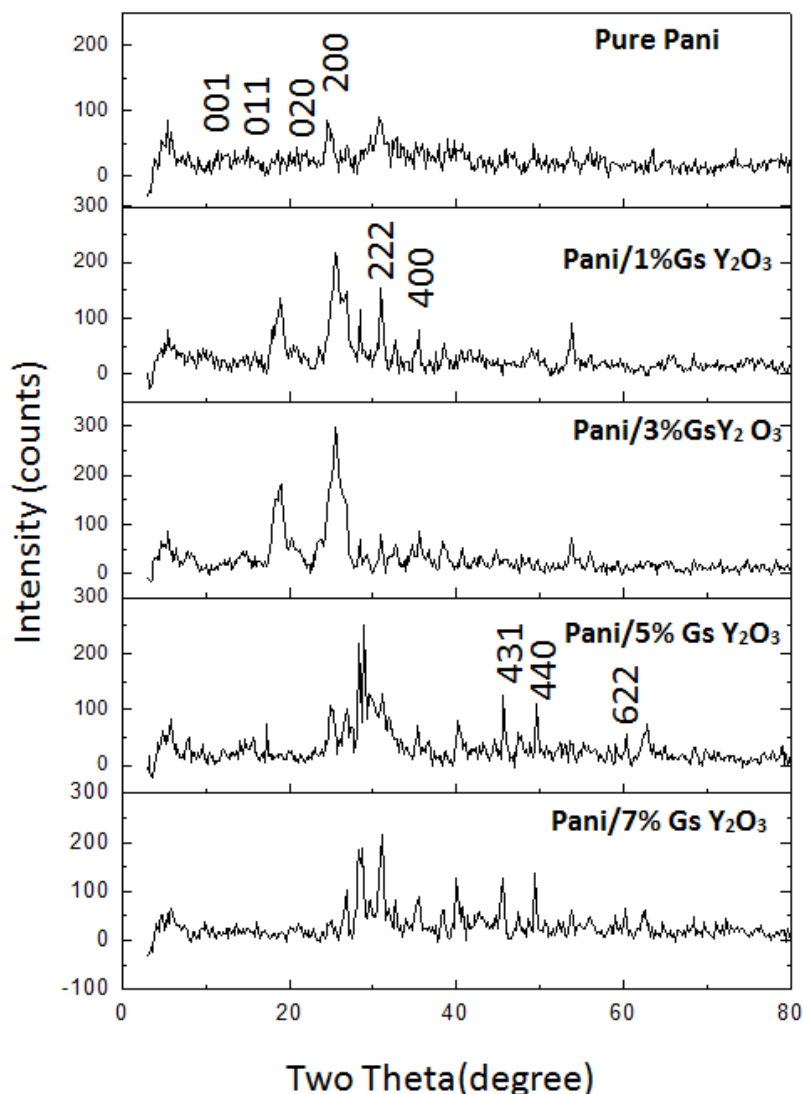


Figure 3: Shows the XRD of pure Pani and Pani/ Gs  $\text{Y}_2\text{O}_3$  nanocomposites

The characteristic sharp peak of Y<sub>2</sub>O<sub>3</sub> planes with d-spacing values in Pani/Gs Y<sub>2</sub>O<sub>3</sub> composite as shown in table 1. Diffraction pattern of the characteristic Pani and characteristic Gs Y<sub>2</sub>O<sub>3</sub> in the composite (1, 3, 5 and 7 weight % of oxide) shows Pani deposited on the surface of Gs Y<sub>2</sub>O<sub>3</sub> particles.

**Table 1: Diffraction planes with 2θ values and inter planar spacing for the Pani and its composites**

Polymer/composites	2 θ values for Pani fibres					2 θ values for Gs Y <sub>2</sub> O <sub>3</sub> fibres with d spacing values				
	001	011	020	200	121	222	400	431	440	622
Pure Pani	9.9	16.0	20.11	25.0	26.4	-	-	-	-	-
Pani/1% Gs Y <sub>2</sub> O <sub>3</sub>	9.2	15.7	19.8	24.9	26.8	29 (3.0)	35.4 (2.5)	45.6 (1.9)	49.5 (1.8)	60.3 (1.5)
Pani/3% Gs Y <sub>2</sub> O <sub>3</sub>	7.8	14.5	19.01	24.3	25.5	25 (3.4)	35.4 (2.5)	44.7 (2.0)	49.7 (1.8)	57.6 (1.5)
Pani/5% Gs Y <sub>2</sub> O <sub>3</sub>	8.2	13.3	18.35	23.6	25.5	25.6 (3.4)	35.4 (2.5)	-	49.0 (1.8)	59.6 (1.5)
Pani/7% Gs Y <sub>2</sub> O <sub>3</sub>	7.7	13.9	19.07	24.6	26.9	31.0 (2.8)	35.4 (2.5)	45.5 (1.9)	49.4 (1.8)	60.0 (1.5)

### 3.4 SEM

Fig. 4(a-e) show SEM of pure Pani and Pani/(1,3, 5 & 7 wt %) Gs Y<sub>2</sub>O<sub>3</sub> composites. SEM images show for Fig 4 a have fibre with lumps Fig. 4b highly fibrous Fig. 4c is lumps with minimum fibre and Fig 4d and 4e clusters of smaller lumps and fibrillar polymer composite. In the above polymer composites show lumps of the Y<sub>2</sub>O<sub>3</sub> with fibrillar Pani forms multi particle aggregates, presumably because of weak interparticle interactions<sup>37</sup>. The formations of nanofibre are well authenticated by using DBSA which enhances the chain length of the polymer<sup>38</sup> at lower weight percentage of Y<sub>2</sub>O<sub>3</sub> nanofiber formation well noticed. Table 2 shows the atomic and weight percentage data for elements C, N, Y and O obtained from EDS spectra for Pani and Pani /Gs Y<sub>2</sub>O<sub>3</sub> nanocomposites. Table 2 shows variation in the percentage of carbon in Pani/Gs Y<sub>2</sub>O<sub>3</sub> nanocomposite sample, which may be attributed to the variation in degree of polymerization. By contrast, the increase in the Gs Y<sub>2</sub>O<sub>3</sub> in the composites decrease in the percentages of C and O may be due to the partial oxidation of Pani Chains during the Pani nanofibers formation. As we have shown in the Fig 2 and 4, suggest that probable involvement of Y<sub>2</sub>O<sub>3</sub> in the Pani/Gs Y<sub>2</sub>O<sub>3</sub> formation.

**Table 2: Atomic and weight percentage data obtained from EDS spectra for Pure Pani and Pani/ Gs Y<sub>2</sub>O<sub>3</sub> nanocomposites**

Element	Atomic %				Weight %			
	C	N	O	Y	C	N	O	Y
Pure Pani	88.91	2.30	-	-	86.07	2.59	-	-
Pani/1% Gs Y <sub>2</sub> O <sub>3</sub>	92.52	2.82	4.52	0.14	89.89	3.19	5.85	1.07
Pani/ 3%Gs Y <sub>2</sub> O <sub>3</sub>	92.03	1.98	5.78	0.21	88.87	2.23	7.43	1.47
Pani/ 5%Gs Y <sub>2</sub> O <sub>3</sub>	90.21	2.91	6.46	0.42	85.21	3.20	8.63	2.96
Pani/ 7%Gs Y <sub>2</sub> O <sub>3</sub>	90.10	2.30	6.98	0.62	84.20	3.20	9.01	3.59

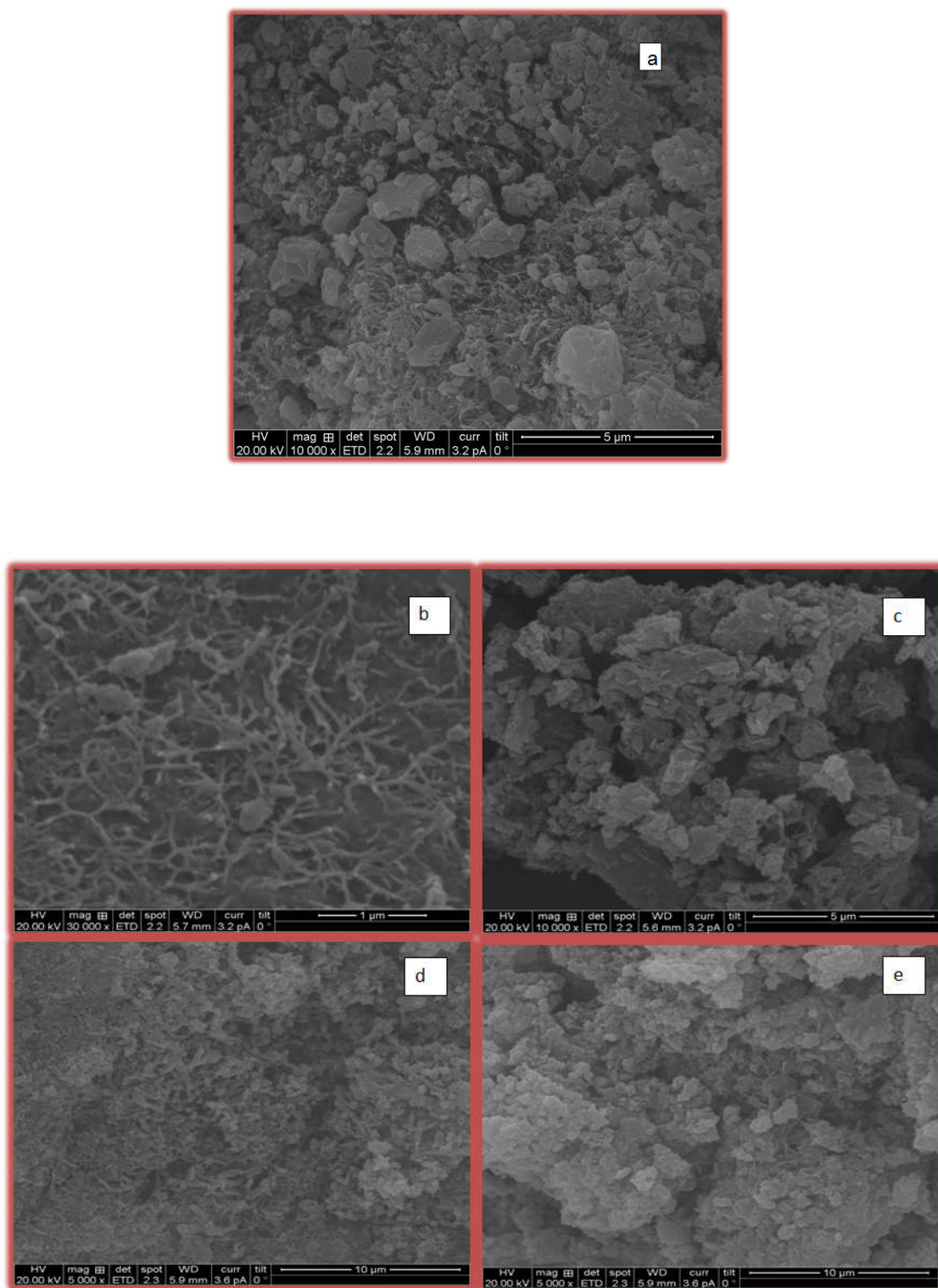


Figure 4: Shows the SEM of (a) Pure PANI (b) PANI/1% Gs  $\text{Y}_2\text{O}_3$ , (c) PANI/3% Gs  $\text{Y}_2\text{O}_3$ , (d) PANI/5% Gs  $\text{Y}_2\text{O}_3$  and (e) PANI/7% Gs  $\text{Y}_2\text{O}_3$  nanocomposites



### 3.5 TEM

Fig. 5 (a, b-e) shows the TEM images of Pani and Pani/(1,3, 5 & 7 wt %) Gs  $\text{Y}_2\text{O}_3$  nanocomposites. The TEM images of Fig. 5a show for pure pani nanofibers forming polymer chain cluster structures. Fig. 5b shows the nanofibers with the thickness of 110 nm and inset of the Fig 5b shows the selected area electron diffraction pattern indicating the diffraction rings for the Gs  $\text{Y}_2\text{O}_3$  with Pani nanofibers.

The TEM images of Pani- Gs  $\text{Y}_2\text{O}_3$  composites from Fig. b-e shows polymer chain cluster with more or less spherical and linkage between the structures. The sizes of the spherical structures are around 100 nm. The spherical structures of Pani/Gs  $\text{Y}_2\text{O}_3$  are similar to that of Pani as reported in literature studies<sup>39</sup>. Yong Ma<sup>20</sup> explains such a spheres with Pani coating on  $\text{Fe}_3\text{O}_4$  microsphere chains as a chain like hallow sphere without using the surfactants. In our results coating of pani nanofibers on the Gs  $\text{Y}_2\text{O}_3$  similar hallow spheres link using DBSA surfactants helps to growth of the link between the hallow spheres.

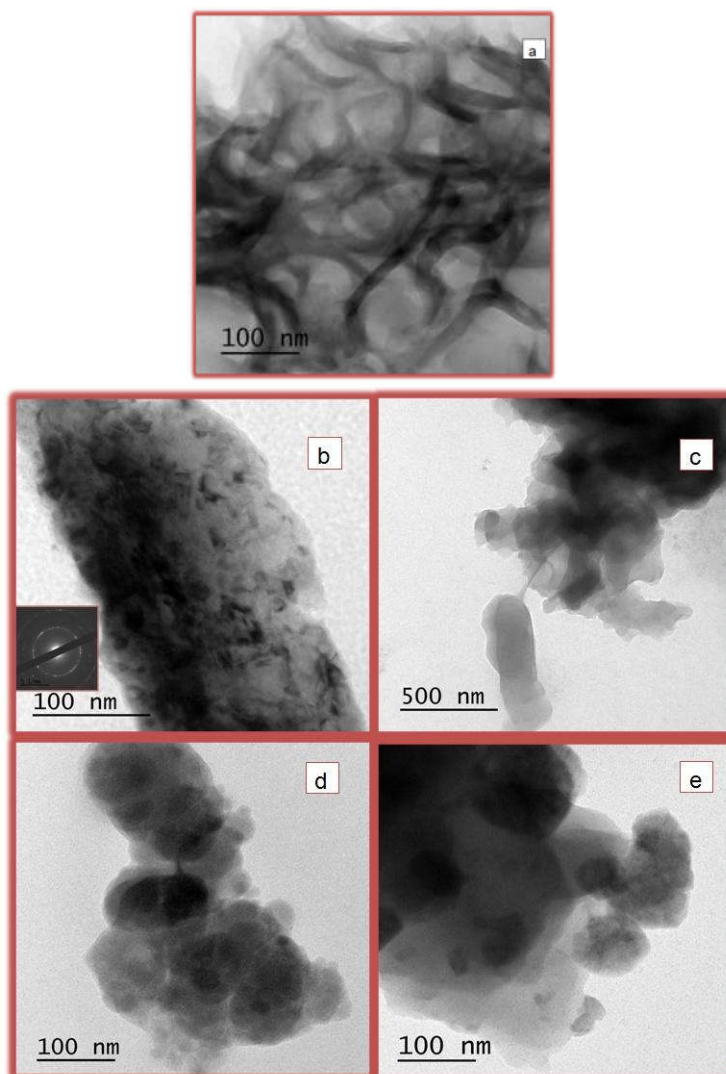


Figure 5: Shows the TEM of (a) Pure Pani (b) Pani/1% Gs  $\text{Y}_2\text{O}_3$ , (c) Pani/3% Gs  $\text{Y}_2\text{O}_3$  (d) Pani/5% Gs  $\text{Y}_2\text{O}_3$  and (e) Pani/7% Gs  $\text{Y}_2\text{O}_3$  nanocomposites inset of b is for selected area electron diffraction pattern

#### 4. Electrical Property

##### 4.1 Conductivity

Fig. 6 shows conductivity as a function of frequency with Pani/ (1 %, 5% and 7%) Gs Y<sub>2</sub>O<sub>3</sub> nanocomposites, inset of the Fig. 6 shows for Pure Pani. The room temperature at 100 Hz frequency dependent conductivity shows highest conductivity than the other composites. Due to the fibrillar and semi crystalline nature of the Pani- Gs Y<sub>2</sub>O<sub>3</sub> composites as indicated by the XRD and SEM. At low frequency all the Pani composite with Pure Pani shows constant conductivity upto 10<sup>3</sup> Hz and slight increase in conductivity between 10<sup>3</sup>-10<sup>5</sup> Hz frequency. After 10<sup>5</sup> - 10<sup>6</sup> Hz frequency range increases and reaches maximum conductivity and then decreases. This change in the ac conductivity may be due to obeying the power law of Jonscher's empirical universal behaviour for the disordered conducting composites<sup>40-42</sup>.

$$\sigma_{ac} \propto \omega^n, \text{-----} 1$$

Variation in the ac conductivity at high frequency region is usually described by variation in the value of n from the above equation (n is constant or less than 1 for the fractional exponent). When Pani/5% Gs Y<sub>2</sub>O<sub>3</sub> shows highest conductivity may be due to highest critical oxidised form and of the aniline shows highest disorderdness. As the further increased addition of the Y<sub>2</sub>O<sub>3</sub> in the Pani also decreases the conductivity may be due to increased orderedness may reflected the decreased conductivity. The disorderd polymer composites may be of various chain lengths forming the conduction network having the polarons and bipolarons as charge carriers. Disorderdness in the composites may be due to different method of synthesis and different doping process of the polymer and its composites<sup>43</sup>. Method of synthesis may variation in the polymer chain length and its composites and addition of the oxide may also affect the intra and inter chain hopping of the conducting path. That resulting in the space charge polarization of the composites contributing the variation in the conductivity<sup>34</sup>. Electronic properties of polymer and its composites are sensitive to the synthetic methods and materials used in the synthesis and mainly dopants and its concentrations.

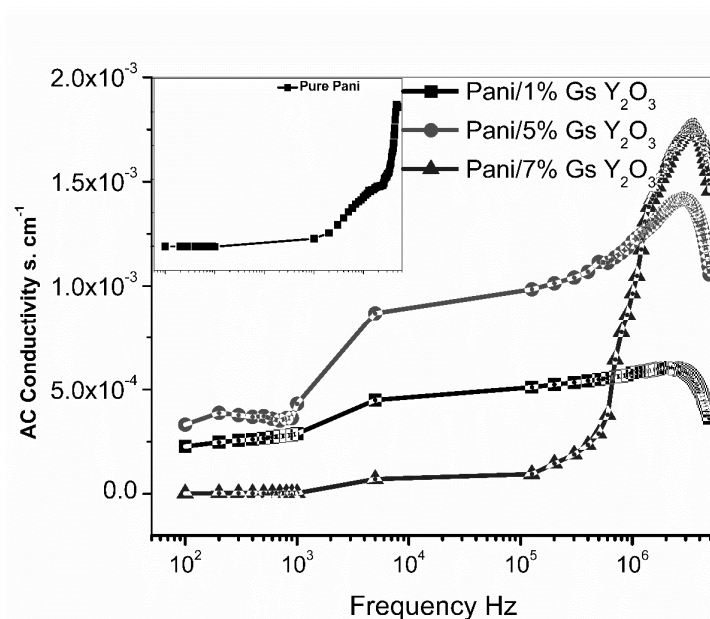


Figure 6: Frequency dependent Ac conductivity of the Pani/ Gs Y<sub>2</sub>O<sub>3</sub>, composites inset shows for pure Pani

#### 4.2 Dielectric Constant

Fig. 7: Shows room temperature dielectric constant as a function of frequency (Hz) for Pani (inset) and Pani/(1%, 5% and 7 %)Gs  $\text{Y}_2\text{O}_3$  composites. Pani/ 5% Gs  $\text{Y}_2\text{O}_3$  at 100 Hz frequency show high values are related to the Pani nanofiber effects of electrode polarization and space charge polarization<sup>34</sup>. Due to the variation in the oxide in the polymer composites affecting the composition, protonation, temperature and delocalization length of the polyaniline resulting in the high dielectric constant<sup>43</sup>. From the Fig. 7 it is observed that for all these composites, as frequency increased from  $10^2$  to  $10^3$  Hz dielectric constant decreased sharply, above  $10^3$  Hz dielectric constant becomes almost persistent for higher frequencies. Mobile polaron/bipolarons of the conducting polyaniline are free to move along the chain, due to the addition of the Gs  $\text{Y}_2\text{O}_3$  in the nanocomposites restricts mobility of the charge carriers resulting in strong polarization in the system. But that of the Pani/5% Gs  $\text{Y}_2\text{O}_3$  nanocomposites there is proper interlink between the Yttria and Pani is maximum resulting in the critical percolation and maximum dielectric constant. Critical percolation may be due to the grain and grain boundary contribution of the Pani/5%  $\text{Y}_2\text{O}_3$  composites resulting in high dielectric constant. That of the other composites predominant grain or grain boundary contribution resulting in lesser dielectric constant values. Thus upon increasing the applied field frequency above the  $10^3$  Hz, the dipoles present in the polyaniline in the composites unable to reorient quickly to respond to the applied field thereby persistent dielectric constant.

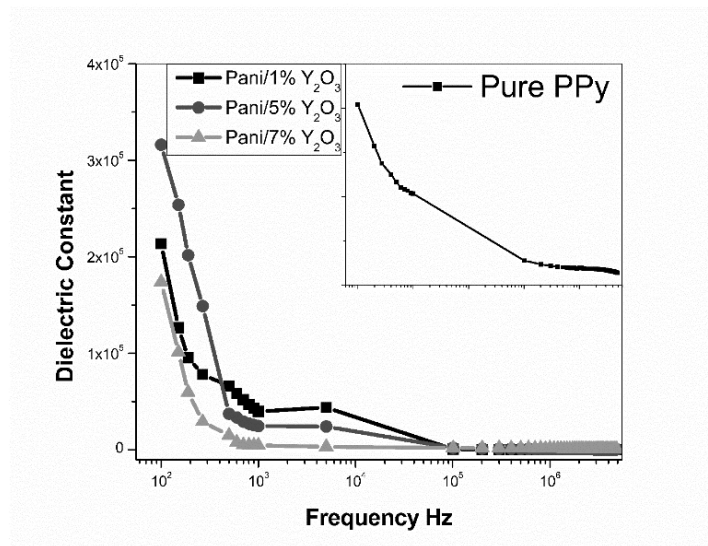
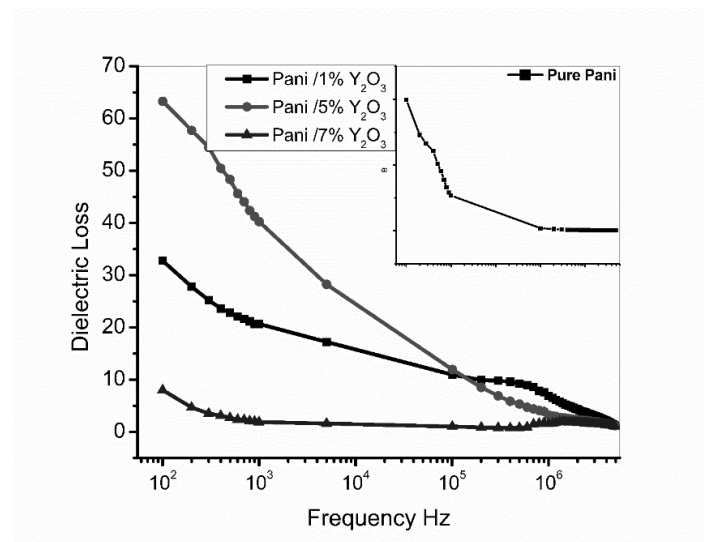


Figure 7: Frequency dependant dielectric constant of Pani/Gs  $\text{Y}_2\text{O}_3$  composites inset shows for pure Pani

#### 4.3 Dielectric Loss

Fig. 8 depicts the dielectric loss values as a function of frequency for Pure Pani (in the inset) Pani- Gs  $\text{Y}_2\text{O}_3$  composites at room temperature. It is observed that the dielectric loss decreases as frequency is increased. At 100 Hz frequency maximum dielectric loss was shown by the Pani/5% Gs  $\text{Y}_2\text{O}_3$  composites. High values of dielectric loss are shown upto  $10^5$  Hz frequency, after that dielectric loss values falls below Pani/1% Gs  $\text{Y}_2\text{O}_3$ . The same trend is also observed in the literature for many polymer composites<sup>22</sup>. They explained such behaviour may be due to highly polar interaction of Pani with dispersed Gs  $\text{Y}_2\text{O}_3$  lead to the different relaxation phenomena of the medium degree of crystallinity for the charge transport.



**Figure 8: Frequency dependant Dielectric Loss for the Pani/Gs  $Y_2O_3$  composites and inset shows for pure Pani**

## 5. Conclusion

Successful synthesis of the Pani/Gs  $Y_2O_3$  oxidised by  $FeCl_3 + APS$  in DBSA surfactant gives Fiber like cluster with Gs  $Y_2O_3$ . The UV visible spectra of the composites show dispersion of high molar mass of the Gs  $Y_2O_3$  in the oxidised form of the polyaniline. FTIR Spectra of the composites show the interactions between pani nanofiber with Gs  $Y_2O_3$  nano particles in the composites. Interplanar d-spacing values for the Pani indicates the nanofiber and broad peak for the amorphous nature of the pani is extracted from the XRD. Sharp peaks at higher  $2\theta$  values indicating the presence of Gs  $Y_2O_3$  in the composite. Presence of the nanofibers of the polyaniline forming the cluster with Gs  $Y_2O_3$  in the composites. Presence of polyaniline fiber with less spherical linkages and formation of the cluster is further fortified by the TEM. AC Conductivity of the composite behaviour is following the Jonscher's universal power law. Variation in the conductivity may be due to disorderedness in the polymer chain length resulting in the formation of charge carriers. Disorderiness may be achieved due to oxidised form of the aniline in the composite or loading of  $Y_2O_3$  in the composites. Highest dielectric constant and dielectric loss behaviour of the composites may be due to the space charge polarization. These polyaniline/ Gs  $Y_2O_3$  composites are more anticipated for suitable EMI shielding, sensor and battery applications.

## References

1. Ramasamy Srinivasan, Rajeswari Yogamalar, Arumugam Chandra Bose *Mat. Res. Bulletin*, 45, 1165. (2010)
2. Guo Huang, Hong Zhanglian, Zhang Shizhu, Zhang Pengyue Fan Xianping *J. of Rare Earths* 24, 47(2006) (Sp. Issue).
3. Xue Bai, Hongwei Song, Lixin Yu, Linmei Yang, Zhongxin Liu, Guohui Pan, Shaozhe Lu, Xingguang Ren, Yanqiang Lei, and Libo Fan *J. Phys. Chem. B* 109, 15236 (2005)
4. Morteza Hajizadeh-Oghaz, Reza Shoja Razavi, Masoud Barekat, Mahdi Naderi, Saadat Malekzadeh, Mohammad Rezazadeh, *Journal of Sol-Gel Science and Technology*, 8, (3) 682(2016).
5. R.V Mangalarajaa, J. Mouzon, P Hedstrom, KeroI. Ramama K.V.S, Carlos P. Camurri, Oden M.J. *of Mat.Processing Tech.* 208 415. (2008)
6. T Mimani. and. K.C Patil *Mater. Phys. Mech.* 4, 134.( 2001)
7. S. K Kannan and M Sundrarajan, *Bul. of Mat. Sci.*, 38, 4, ,945(2015)

8. N.J Shivaramu, B.N Lakshminarasappa, K.R Nagabhushana, Fouran Singh, *Spectrochimica Acta Part A: Molecular and Biomolecular Spectroscopy*, 154220. (2016)
9. Soo-Muk Cho, Kab-Yeul Jang, Hong Ju Park, and Jeong-Sik Park, *Mycobiology*. 36(1): 50. (2008)
10. Jagpreet Singh, Tanushree Dutta, Ki-Hyun Kim, Mohit Rawat, Pallabi Samddar and Pawan Kumar, *J. of Nanobiotech.*,16:84.(2018)
11. M Chandrasekhar. H Nagabhushana. K.H Sudheerkumar,. N, Dhananjaya. S.C Sharma, D Kavyashree, C Shivakumara, B.M Nagabhushana., *Mat. Res. Bul.* 55, 237(2014)
12. RJose. Peralta-Videa, Yuxiong Huang, G Jason. Parsons, Lijuan Zhao, Laura Lopez, AMoreno Jose. L Hernandez-Viezcas, Jorge. Gardea-Torresdey, *Nanotech. For Environ. Engg.*, 1, 4. (2016)
13. Narasimha Golla, B Praveen, K Mallikarjuna B, Deva Prasad Raju *Int.J.Nano Dim.*2(1): 29(Summer)( 2011)
14. Manzoor-ul-Haq, Vandana Rathod, Dattu Singh, Ashish Kumar Singh, Shivaraj Ninganaagouda and Jyothi Hiremath, *Nanosci. and Nanotech. An Inter.J.*, 5(1)1(2015)
15. KB Satishkumar, TK Vishnuvardhan B, Rajashekhar, K Satish, Shashidhar, and B Sreekanth, *Asian J. of Chem.* 31(4)834.( 2019)
16. M Mohamad. AAyad, Wael. Amer, Mohamad Whdan, *J.of App. Poly.Sci.*125, 2695(2012)
17. Abdel Aziz Rahy, Mohamed Sakrout, Sanjeev Manohar, Sung June Cho, John Ferraris, and D. J. Yang, *Chem. Mater.* 20, 4808(2008)
18. Shiow-Jing Tang, Ku-Yen Lin, Yun-Rong Zhu, Hsiu-Ying Huang, Wei-Fu Ji, Chun-Chuen Yang, Yu-Chiang Chao, Jui-Ming Yeh and Kuan-Cheng Chiu, *J. Phys. D:Appl. Phys.*46,505301 (2013)
19. Wen-Yi Su, Feng-Yan Liang& Li Ma, *Int. J. of Poly. Anal. Charact.* 17: 93,( 2012)
20. Yong Ma, Mingtao Qiao, Chunping Hou, Yanhui Chen, Mingliang Ma, Hepeng Zhang and Qiuyu Zhang, *RSC Adv.*, 5, 103064. (2015)
21. M. Saeed, Abdul Shakoor, Ejaz Ahmad, *J Mater Sci: Mater Electron*,24,3536.( 2013)
22. Muhammad Faisal and Syed Khasim, *Bull. Korean Chem. Soc.*34,( 1) 99.( 2013)
23. E Kowsariand G Faraghi. *Ultrasonic Sonochemistry*17, 718-725.( 2010)
24. T.K Vishnuvardhan, V.R Kulkarni, C. Basavaraja and S.C Raghavendra *Bul. of Mat.Sci.*29(1), 77(2006)
25. Qilin Cheng, Vladimir Pavlinek, ChunzhongLi, Anezka Lengalova, Ying He, Petr Saha, *App. Surf. Sci.*253 1736(2006)
26. K. R Nemade, S.A Waghuley, *Inter. J. of Mod.Phy: Conference Series*, 22380(2013)
27. A.G MacDiarmid, J.C Chiang, A.F Richter and A.J Epstein, *Synth. Met.*, 18 285(1987)
28. J Stejskaland. P Kratochvf, N Radhakrishnan, *Synth. Metals*,61, 225(1993)
29. A.G Mac Diarmid, *Proceed. Nobel Symposium 81*, W.R. Salaneck and I. Lundstr6m, Eds., Oxford Scientific Press, UK, (1992).
30. P. Kratochvf A.D. Jenkins (ed.), *Classical Light Scattering from Polymer Solutions*, *Polymer Science Library* 5, Elsevier, Amsterdam.( 1987)
31. J Stejskal, ARiede, D Hlavata. J Prokes. M, Helmstedt, P. Holler *Synth. Met.*, 96,55(1998)
32. M.E Jozefwicz., R Laversanne. H.H.S, Javadi, A.J. Epstein, J.P Pouget, X Tang,. A.G MacDiarmid, *Phys. Rev.B*, 39, 12958(1989)
33. J Jiang,. L. H. Ai, D. B Qin,. H. Liu, L. C Li,. *Synth. Met.* 159, 695(2009)
34. Z. Zhang, Z.Wei, M.Wan, *Macromolecules*, 35, 5937. (2002)
35. R E Partch, S G Gangoli, E Matijevic, W Cai and S Arajjs. *Colloid. Interface Sci.* 27 144 (1991)
36. J Ouyang and Y Li *Polymer* 38 3997(1997)
37. M Abdul Shakoor, M Tariq Bhati, Farooq, Iftakhar Paracha *Pensee Journal*, 176, (7)162(2014)
38. Ali olad, FahimehIlghami, Rahimeh Nosrati, *Chemical Papers*, 66(8), 757(2012)
39. Te-Cheng Mo, Hong-Wen Wang, San-Yan Chen, Yun-ChiehYeh, *Cer. Inter.*341767(2008)
40. Papathanassiou, A. N. Sakellis, I. Grammatikakis, *J. Appl. Phys. Lett.* 91,122911(2007)
41. C. R Bowen, A.C. E Dent, D. P Almond, T. P Comyn,. *Ferroelectrics*, 370 166. (2008)
42. A.N. Papathanassiou, I Sakellis, J Grammatikakis,. S. Sakkopoulos, E Vitoratos,. E Dalas, *Synth. Met.* 42 81(2004)
43. S.M Yang. K. H Chen, *Synth. Met.* 135,51. (2003)